

Rapid formulation of redox-responsive oligo- β -aminoester polyplexes with siRNA via jet printing

"Received 00th January 20xx,
Accepted 00th January 20xx

Tatiana Lovato^{a†}, Vincenzo Taresco^{a†}, Ali Alazzo^a, Caterina Sansone,^b Snjezana Stolnik,^a Cameron Alexander^{a*} and Claudia Conte.^{a,b*}

DOI: 10.1039/x0xx00000x

www.rsc.org/

Here we describe a rapid inkjet formulation method for screening newly-synthesised cationic materials for siRNA delivery into cancer cells. Reduction responsive oligo- β -aminoesters were prepared and evaluated for their ability to condense siRNA into polyplexes through a fast inkjet printing method. A direct relationship between the oligomer structures and charge densities, and the final cell response in terms of uptake rate and transfection efficacy, was found. The oligo- β -aminoesters were well-tolerated by the cancer cells, compared to conventional cationic polymers so far employed in gene delivery, and were as active in silencing of a representative luciferase gene.

Introduction

Successful and practical gene therapies require consistent formulations which can be easily prepared, and which can effectively deliver nucleic acids to intracellular target sites.^{1, 2} In turn these formulations need nucleic acid carrier vehicles which are safe in human patients, and with the highest performance in terms of *in vivo* stability, cellular delivery and transfection efficiency.³ Accordingly, combinations of advances in materials chemistry and pharmaceutical formulations are pre-requisites for nucleic acid therapeutics.⁴

To date, the formulation parameters for nucleic acid delivery have generally evolved from research lab-based protocols for preparing polymer-nucleic acid polyelectrolyte complexes, and these can be highly 'operator-dependent'. In part this is due to the many variables important in the polycation carrier /nucleic acid polyanion association process, as the kinetics of polyelectrolyte complex formation are highly variable across concentration ranges, order and speed of addition.⁵⁻⁸ As a consequence, methods to prepare, formulate and screen cationic polymers for nucleic acid delivery are required, and these protocols need to be rapid, use small quantities and be easily applicable across ranges of physical and chemical properties. The increasing use of printing methods for screening pharmaceutical materials is a potential means by which polymer-nucleic acid complexes might be optimised for practical formulations.⁹⁻¹¹

Concurrently, a very wide range of natural and synthetic cationic polymers have been explored as potential non-viral gene delivery systems, particularly for cancer treatment.¹ Amongst these materials, oligo- and poly(β -aminoester)s (OBAEs and PBAEs) have emerged as promising candidates, as they are easy to synthesise and are biodegradable due to their hydrolysable ester backbones.^{12, 13} These materials are generally positively charged at physiological pH and thus are

able to condense spontaneously with nucleic acids through electrostatic interactions. The main advantage of PBAEs compared to other conventional cationic materials is their significantly lower cytotoxicity, combined with their ability to transfect cells with high efficiency^{14, 15}. However, the molecular weight, the structure and the supramolecular architectures of polycations, including PBAEs, play a pivotal role in the final biological effect, influencing the cytotoxicity as well as the gene transfection activity¹⁶⁻²⁰. For instance, it has been demonstrated that polycations with high molecular weight (MW) usually show appreciable cytotoxicities, even though their stronger condensation capacity toward nucleic acids tends to improve transfection potency compared to their lower molar mass analogues.^{21, 22} In addition, dependent on their ratio of primary, secondary and tertiary amines, OBAEs and PBAEs may display appropriate pKa ranges to exploit the "proton sponge mechanism" thus enhancing escape of polyplexes and nucleic acids from endosomal compartments which in turn improves access to the targeted genes.^{18, 23, 24} However, while highly stable polymer-DNA complexes are desirable during the initial stages of the delivery process, the release of the nucleic acid cargo is more rapid if the vector can be degraded into smaller, less charged, fragments. The hydrolysis of the polyester backbones in PBAEs in cellular fluids typically occurs on the time scale of several hours to a few days, depending on the polymer structure, thus affecting the release of the gene cargoes and the final transfection effect. While it is possible to tune the degradation rate of the PBAE polymer via molar mass and monomer structure, it is also desirable to encode "on-demand" cargo release, such that very rapid dissociation of the nucleic acid can occur at the correct cellular region. This can be achieved by incorporating disulfide bonds in the polymer backbone, which can be cleaved in the reducing environments of certain intracellular milieu, thereby improved the efficiency of gene delivery.^{25, 26}

In this manuscript, we report the synthesis of a small range of redox responsive, cytocompatible oligo- β -aminoesters (OBAEs) which are able to condense and transfect siRNA into cancer cells. Through a specific modulation of the molar ratio between the starting materials, we obtained OBAEs with different structures and positive charge densities, thus tuning their capabilities to interact with siRNA and elicit a subsequent biological response. Furthermore, we designed the OBAEs to have solubility properties allowing them to be formed into-

^a Division of Molecular Therapeutics and Formulation, School of Pharmacy, University of Nottingham, NG7 2RD, UK.

^b Drug Delivery Laboratory, Department of Pharmacy, University of Napoli Federico II, Via Domenico Montesano 49, 80131 Napoli, Italy

[†] These authors contributed equally; *corresponding authors.

siRNA polyplexes via an easy, fast and cheap inkjet technology. We considered inkjet printing to be particularly suitable for screening the formulations of biotherapeutics in this study as this technique is versatile, scalable and can deposit picolitre volumes of solution with high accuracy and reproducibility. The data together show that oligomeric cations and siRNA can be easily print-formulated into effective in vitro nucleic acid delivery systems.

Experimental

Materials

All solvents were of analytical or HPLC grade and purchased from Sigma or Fisher Scientific unless otherwise stated. Deuterated solvents were from Sigma. Acryloyl chloride, ethylene-dioxy-bis-ethylamine, triethylamine (TEA), dithiodiethanol, sodium chloride, potassium phosphate dibasic and potassium phosphate monobasic, sodium azide, sodium phosphate dibasic, ethidium bromide (EtBr), fluorescamine, polyethylenimine (PEI) (25kDa, branched) calf thymus DNA and glutathione (GSH), were used as received from Sigma Aldrich. Luciferase siRNA (CCGCAAGAUCGCGAGAUU) was provided by Eurogentec (UK). Luciferase Assay System with Reporter Lysis Buffer and CellTiter 96[®] AQueous One Solution Cell Proliferation Assay (MTS) were provided by Promega (UK). Silencer™ Cy™3-labeled Negative Control was provided by ThermoFisher Scientific (UK).

Synthesis and characterization of cationic oligo (β -amino ester)

The synthesis of the oligo- β -amino ester (OBAE) was via a two-step reaction, i.e. the synthesis of disulfanediybis(ethane-2,1-diyl) diacrylate and 2) the Michael addition reaction between disulfanediybis(ethane-2,1-diyl) diacrylate and ethylenedioxy-bis-ethylamine.

(1) Synthesis of disulfanediybis(ethane-2,1-diyl) diacrylate (DSD). Synthesis of DSD was carried out via a literature method with minor modifications.²⁷ Briefly, dithiodiethanol (10 g, 0.065 mol) was added to a round-bottom flask equipped with three-way stopcocks connected to either a nitrogen line or a vacuum pump, and dried via azeotropic distillation with anhydrous toluene (3 x 20 mL) under reduced pressure. After complete evaporation of toluene, anhydrous THF (20 mL) was added via a syringe under inert atmosphere. TEA (6.5 g, 0.065 mol) was added to the solution which was maintained at 4 °C during drop wise addition of acryloyl chloride (3.5 g, 0.039 mol). The solution was allowed to warm to room temperature under magnetic stirring and left to react overnight. The solution was finally filtered to remove the chloride salt of TEA and the crude product was recovered by evaporation of THF. The product was purified by passing through silica column chromatography using petroleum ether/ ethyl acetate 90:10 as eluents to generate a soft solid (yield 85%).

ATR-IR: ν (cm⁻¹) 3449, 2978, 2874, 1725, 1634, 1620, 1513, 1454, 1408, 1371, 1223, 1177, 1045, 978, 911, 814, 663.

¹H NMR (400 MHz, d⁶-DMSO, ppm): δ_{H} 3.01-3.03 (t, 2, J = 8 Hz, -SSCH₂CH₂O-), 4.35-4.38 (t, 2, J = 4 Hz, -SSCH₂CH₂O-), 5.95 (dd, 1,

J = 4 Hz, J = 8 Hz, -OCOCHCH₂), 6.17 (dd, 1, J = 8 Hz, J = 16 Hz, -OCOCHCH₂), 6.36 (dd, 1, J = 4 Hz, J = 20 Hz, -OCOCHCH₂)

¹³C NMR (400 MHz, d⁶-DMSO, ppm): δ_{C} 36.4 (s, 1, -SSCH₂CH₂O-), 62.1 (s, 1, -SSCH₂CH₂O-), 128.1 (s, 1, -OCOCHCH₂), 131.8 (s, 1, -OCOCHCH₂), 165.0 (s, 1, -OCOCHCH₂).

(2) Synthesis of oligo- β -aminoesters (OBAs). For the Michael addition reaction, different amounts of DSD (0.76 mmol, 0.96 mmol, 1.15 mmol) dissolved in 1 mL of anhydrous DCM were added into a solution of ethylene-dioxy-bis-ethylamine (0.17 g, 1.15 mmol) in 1 mL of anhydrous DCM. The reaction was performed in the dark at 30 °C for 5 days under nitrogen. The final product was then dissolved in MeOH and precipitated into ice-cold diethylether three times. Finally, the polymer was dried under vacuum overnight. The yield of the polymer was 72%.

ATR-IR: ν (cm⁻¹) 3269, 3070, 2865, 1643, 1551, 1494, 1457, 1355, 1295, 1099, 1024, 819, 755.

¹H NMR (500 MHz, d⁶-DMSO, ppm): δ_{H} 2.50-2.53 (m, 2, -OCOCH₂CH₂-), 2.72-2.79 (m, 2, -NCH₂CH₂O-), 2.78-2.81 (t, 2, J = 15 Hz, -SSCH₂CH₂O-), 2.94-3.04 (m, 2, -OCOCH₂CH₂-), 3.21-3.24 (m, 2, -OCH₂CH₂NH₂), 3.41-3.44 (m, 2, -OCH₂CH₂NH₂), 3.54-3.57 (m, 2, -NCH₂CH₂O-), 3.58-3.60 (m, 4, -OCH₂CH₂O-, -OCH₂CH₂O-), 3.61-3.63 (m, 2, -SSCH₂CH₂O-), 8.27 (br, 3, -OCH₂CH₂NH₃⁺).

¹³C NMR (500 MHz, d⁶-DMSO, ppm): δ_{C} 32.4 (s, 1, -OCOCH₂CH₂-), 39.0 (s, 1, -OCH₂CH₂NH₂-), 41.5 (s, 2, -SSCH₂CH₂O-), 44.3 (s, 1, -OCOCH₂CH₂-), 51.4 (s, 1, -NCH₂CH₂O-), 60.1 (s, 2, -SSCH₂CH₂O-), 69.4 (s, 2, -OCH₂CH₂O-, -OCH₂CH₂O-), 69.8 (s, 1, -OCH₂CH₂NH₂-), 70.0 (s, 1, -NCH₂CH₂O-), 170.3 (s, 2, -OCOCH₂CH₂-).

m/z found [M-H]⁻: (A):2331 ; (B): 1434; (C): 560

Characterization of OBAs

¹H-, ¹³C-NMR, 2D-NMR (COSY, HSQC, HMBC) spectra were recorded at 25 °C on a Bruker Advance III 500 MHz spectrometer. All chemical shifts are reported in ppm (δ) relative to tetramethylsilane or referenced to the chemical shifts of residual solvent resonances. Multiplicities are described with the following abbreviations: s = singlet, br = broad, d = doublet, t = triplet, m = multiplet, dd = doublet of doublets. Chemical shifts were assigned in parts per million (ppm). MestReNova 6.0.2 copyright 2009 (Mestrelab Research S. L.) was used for analysing the spectra.

FT-IR spectra were recorded with an Attenuated Total Reflection spectrophotometer (Agilent Technologies Cary 630 FTIR) equipped with a diamond single reflection ATR unit. Spectra were acquired with a resolution of 4 cm⁻¹ by co-adding 32 interferograms, in the range 4000-650 cm⁻¹.

IR analysis were performed by using SpectraGryph version1.0.

Mass spectra were carried out using a Micromass LCT ToF with electrospray ionization and OpenLynx software.

Fluorescamine assays for amine content determination

The intensity of fluorophore resulting from the reaction of fluorescamine with primary amine was measured using a Cary Eclipse Fluorescence Spectrophotometer and glycine as standard. To a 2 ml sample of polymer solution (concentration 10 $\mu\text{g}\cdot\text{ml}^{-1}$, in borate buffer pH 8.7), 0.5 ml of fluorescamine in acetone (0.3 $\text{mg}\cdot\text{ml}^{-1}$) were added and vortexed for 10 seconds. After incubation of the reagents in the dark for 20 minutes, the

emission from the resulting solution was measured at a wavelength of 480 nm using an excitation wavelength of 385 nm against a blank of borate buffer with fluorescamine.

Buffer capacity of OBAE

The buffer capacity of OBAE was determined by acid-base titration. Acid-base titration was performed using a Fisherbrand pH meter with a Hydrus 600 electrode. Briefly, 0.5 mg of PBAE were dissolved in 1 mL of NaCl 0.1 M and the pH of the polymer solution was adjusted with 0.1 M HCl to 3. Then, the solution was titrated with NaOH 0.1 M and the pH value of solution was measured.

The buffering capacity was defined as the percentage of the protonated amine groups from pH 7.4 to 5.0 and calculated according to the following equation:

$$\text{Buffer capacity (\%)} = 100 (\Delta V_{\text{NaOH}} \times 0.1\text{M}) / N \text{ mol}$$

Where, ΔV_{NaOH} is the volume of 0.1M NaOH, which changes the pH of the polymer sample from 5 to 7.4, and N mol is the total moles of amine groups in the sample.

For total amine content, the volume of NaOH required to ionize all the amine groups based on the first derivative analysis of titration curve was used and multiplied by the concentration (0.1 M). As the concentration of NaOH is the same, it can be removed from the above equation.

Printing set-up and work flow conditions

Prior to dispensing the siRNA aqueous solutions into a 96-wellplate filled with 100 μL of water solutions of OBAs for each well, the target had to be defined. Firstly, the outer dimensions of the wellplate were added to the software scifLEXARRAYER (Sciencion AG, version 2.09.002) followed by defining the number of wells, well distance, well depth and the spot area (area within the target designated for spotting). siRNA solutions were dispensed via a piezo electric inkjet printer (Sciflexarray S5, Sciencion) through a 90 μm orifice nozzle. Each droplet was dispensed with a rate of 30-40 drop/ μs with sizes ranging in between 250 and 280 pL. Droplet volume was altered by tuning the values of the voltage (98-105 Volt) and electrical pulse (45-55 μs). Images of the drop formation and droplet size were obtained using the printer software. The final spots were imaged using the Leica MZ16 stereomicroscope.

Depending on the siRNA/oligomer ratios to be reached, the number of drops per spot was adjusted accordingly. The nozzle was washed with Milli-Q water, in between each printing cycle, as part of the automated printing-washing loop. The nozzle was programmed to dispense the siRNA solutions into the well from a vertical distance of *circa* 10-20 mm from the well-plate, no contact between the nozzle tip and the water surface was allowed.

Polyplexes characterization

The hydrodynamic diameter (DH), polydispersity index (PI) and zeta potential of polyplexes were determined on a Zetasizer Nano ZS (Malvern Instruments Ltd.). A NP dispersion was

diluted in Milli-Q water at intensity in the range 10^4 - 10^6 counts/s and measurements were performed at 25°C on 90° angle. Results are reported as mean of three separate measurements of three different batches ($n=9$) \pm standard deviation (SD). Morphology and shape of polyplexes were monitored through Atomic Force Microscopy (Bruker Dimension Fast Scan Bio).

siRNA complexation was confirmed by agarose gel retardation. Polyplexes containing 1 μg of siRNA were loaded on 2% agarose gel in Tris-Acetate-EDTA (TAE) buffer and subjected to electrophoresis for 45 min at 70 V. siRNA bands were stained with EtBr and finally visualized with an UV illuminator.

Ethidium bromide displacement assay

In this assay, Calf thymus DNA (50 $\mu\text{g}/\text{mL}$ in PBS) was incubated with ethidium bromide (2 $\mu\text{g}/\text{mL}$) for 30 minutes. Thereafter, aliquots of 100 μL were mixed with 100 μL of polymer solutions at different concentrations. The samples were incubated under stirring for 30 minutes, and then the fluorescence intensity of DNA-Ethidium bromide complexes was measured at a wavelength of 590 nm using an excitation wavelength of 520 nm.

Cell culture

A549 lung cancer cells were obtained from the American Type Culture Collection, cultured at 37°C in a humidified atmosphere containing 5% CO_2 and grown continuously in DMEM supplemented with 10% FBS, 100 unit/mL penicillin and 100 $\mu\text{g}/\text{mL}$ streptomycin.

Cell metabolic activity (viability) assay

A549 luciferase expressing cells (2×10^4) were placed in 96-well plates and cultured in 200 μL of cell medium with or without FBS at 10%. After 24 h, cells were treated with free OBAs in the concentration range 0.005-5 mg/mL. As control, cells were treated as well as with an aqueous solution of free Polyethylenimine (PEI) at the same concentration range. Cells treated with 0.1% (v/v) Triton-X 100 and fresh media were used as a positive and a negative control, respectively. After 24 h of incubation, cells were washed with PBS and treated with CellTiter 96® Aqueous One Solution Cell Proliferation Assay (MTS, Promega) (20 μL per well). After further incubation (3 h), the absorbance was read at 490 nm in a microplate reader (Tecan Platereader). The percentage of metabolic activity (%) was calculated according to the equation:

$$\text{Cell viability (\%)} = [(\text{OD sample} - \text{OD CTR+}) / (\text{OD CTR-} - \text{OD CTR+})] \times 100$$

Transfection studies

For transfection studies, A549 luciferase expressing cells (5×10^4) were seeded into 24-well plates and cultured in 500 μL of cell medium with FBS at 10%. After 24h, the culture medium was replaced with 0.5 mL of fresh serum-free DMEM and treated with siRNA/OBAE polyplexes containing 1 μg of siRNA/well. After 4h of incubation, cells were washed three

times with fresh medium in order to remove NPs and incubated again at 37°C until 48h. Finally, after transfection, luciferase activity was measured as RLU/mg protein using the luciferase assay system (Luciferase Assay System with Reporter Lysis Buffer, Promega) and BCA reagent (Sigma, UK).

Uptake and Endolysosomal escape

A549 luciferase expressing cells (2×10^4) were seeded in eight well chamber slides (Nunc, Thermo Fisher Scientific Inc., UK) and cultured in 300 μ L of cell medium with FBS at 10%. After 24 h, the culture medium was replaced with 0.3 mL of fresh serum-free DMEM and treated with 10 mg/mL of polyplexes formed by OBAEs and Cy3-siRNA at 10:1 polymer/siRNA weight ratio. After 4h of incubation, cells were washed three times with fresh medium without Phenol Red and treated with LysoTracker Green DND-26 (Invitrogen Life Technologies, UK) containing media (100nM) and then with DAPI (Invitrogen Life Technologies, UK) containing media (1 μ g/mL) for 10 minutes at rt in the dark according to the manufacturer's specifications. Live cells were finally imaged through confocal microscopy (Zeiss LSM 700 Confocal Laser Scanning Microscope equipped with Argon and HeNe lasers and a 40X/1.2 NA water objective). Zen 2009 image Software was utilized for image processing.

Statistical analysis

Unless otherwise stated, all data are shown as mean \pm standard deviation (SD), two-way analysis of variance (ANOVA) was applied for comparison of three or more group means (Tukey's multiple comparisons test). P value of <0.05 was considered statistically significant. ****, ***, **, and * display $p < 0.0001$, $p < 0.001$, $p < 0.01$, and $p < 0.05$, respectively. GraphPad Prism 6 software was used for data analysis.

Results and discussion

The initial focus for the study was to develop oligomers and polymers with properties suitable for rapid condensation of siRNA via inkjet printing and also triggered degradation properties. Accordingly, OBAEs were synthesized through Michael-type addition reaction between the acrylate groups of a disulfanediylbis(ethane-2,1-diyl) diacrylate (DSD), and the terminal amino groups of ethylene-di-oxy-bis-ethylamine.

The bioreducible disulfide-containing monomer DSD was synthesized through reaction of dithiodiethanol with acryloyl chloride and its structure confirmed by ^1H , ^{13}C and 2D-NMR spectroscopy (Fig. S1), as previously reported²⁷. Then, DSD was employed in a Aza-Michael addition reaction with the diamine ethylene-bioxy-bis-ethylamine, using different molar ratios of the starting materials (1:1, 1:1.25 and 1:1.5 DSD/ ethylene-di-oxy-bis-ethylamine ratio), thus yielding three different OBAEs (A, B and C, respectively). The ratios of the diacrylate and diamine were varied in order to modulate the final properties

of the products. The higher diamine ratio was intended to produce a lower molar mass product and the 1:1 mixture the highest molar mass, which we anticipated would affect their 'printability'.

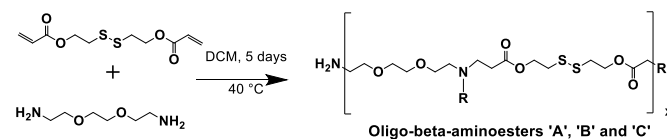
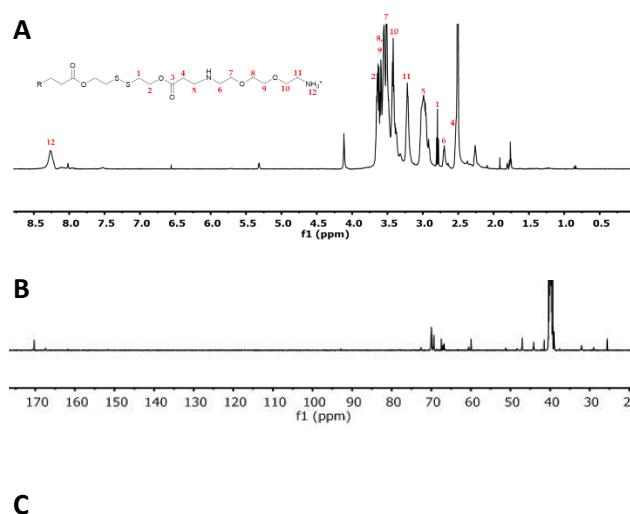


Figure 1: Synthetic reaction of OBAEs.

The condensation reactions were allowed to proceed for 5 days at 30 °C (Fig. 1). All the OBAEs synthesized were characterized through ^1H , ^{13}C and 2D-NMR spectroscopy in d_6 -DMSO (Fig. 2, S2 and S3), Electron Spray Ionization (ESI) mass spectra (Fig. S5) and FT-ATR-IR spectroscopy (Fig. S6).

The ^1H -NMR spectra of the three OBAEs synthesised gave very similar NMR spectra (Fig. 2, S2A and S3A). In particular, the resonances of the protons of the methyl groups at $\delta=2.25$ -2.27 ppm and $\delta=2.90$ -3.02 ppm (n. 5 and 6 respectively) confirmed the presence of a secondary amine in the OBAE backbone. The signal of the protons of the methyl groups adjacent to the disulfide bond at $\delta=3.41$ -3.43 ppm (n. 1) demonstrated the integrity of the disulfide bond after the reaction with ethylene-di-oxy-bis-ethylamine. The lack of a resonance at $\delta=5.00$ -7.00 ppm associated with the vinyl protons denoted complete conversion of the terminal double bonds during the Michael addition reaction and the presence of a peak at $\delta=8.27$ ppm indicated a protonated primary amine at the chain terminus. However, it is possible to notice in Fig. S4 that the relative intensities of the signals of the proton adjacent to the disulphide bond (yellow circle) and the protons in proximity of the newly formed secondary amine (pink circle) changes. This change was not proportional to the variation in feed ratio of ethylene-di-oxy-bis-ethylamine and could be explained by hydrolysis of the ester bond on inter/intra molecular amidation reaction occurring between NH_2 and ester bond in line with ^{13}C and 2D-NMR spectroscopy.



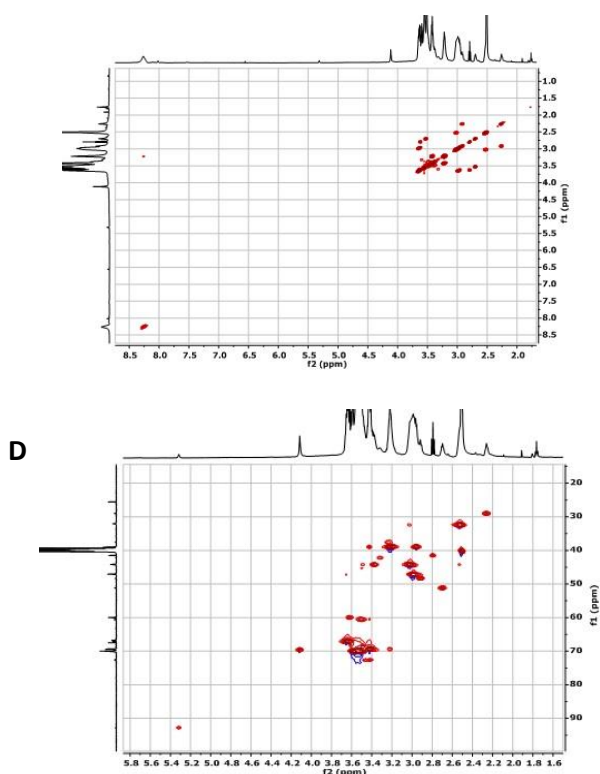


Figure 2. Characterization of OBAE C. A) ^1H NMR spectrum; B) ^{13}C NMR spectrum collected for 6h; C) ^1H - ^{13}C COSY NMR spectrum and D) ^1H - ^{13}C HSQC NMR spectrum. Spectra recorded at 500 MHz in d_6 -DMSO.

Due to the intrinsic chemical similarity in terms of functionalities, the three OBAEs showed essentially superimposable ATR-IR spectra as evidenced in figure S6. FT-ATR-IR spectra of the OBAEs showed a broad signal at 3250 cm^{-1} , typical of the stretching resonance of an extended H-bonded network of both secondary and primary amine groups, in contrast to the two sharp peaks at 3400 cm^{-1} and 3200 cm^{-1} in the spectrum of ethylene-dioxy-bis-ethylamine starting material due to primary amine functionality. The formation of a secondary amine was also confirmed by the shift of the N-H bending resonance from 1595 cm^{-1} to 1551 cm^{-1} . The frequency of the C=O stretching band moved from 1725 cm^{-1} in the spectrum of DSD to 1643 cm^{-1} in the spectrum of OBAEs, as a result of the Michael addition reaction. Additionally, as for DSD, OBAEs showed a weak transition at around 670 cm^{-1} characteristics of C-S stretching.

ESI mass spectroscopy suggested molar masses ranging from 560 Da (OBAE C, Figure S5C) to 1434 Da (OBAE B, Figure S5B) and 2331 Da (OBAE A, Figure S5A) for the OBAEs synthesized, as expected from a step growth polymerization under the conditions employed. GPC data were difficult to interpret, perhaps owing to adsorption of the oligomers to the columns used, and thus additional characterisation methods were required. The number of reactive primary amines on the OBAEs were determined by fluorescamine assays, and the total number of basic amines was determined by acid-base titration (Fig. S7). The values for the amine content of the oligomers were A: 0.85 mmol/g; B 1.39 mmol/g and C: 3.27 mmol/g. These results were in excellent agreement with fluorescamine assay

data for OBAE C (also 3.27 mmol/g), but less well-correlated for A and B, most likely due to their lower overall amine content. Taken together, these data suggested a series of different materials, for which the theoretical structures derived from the most common fragments detected in mass spectrometry are shown in figure 3.

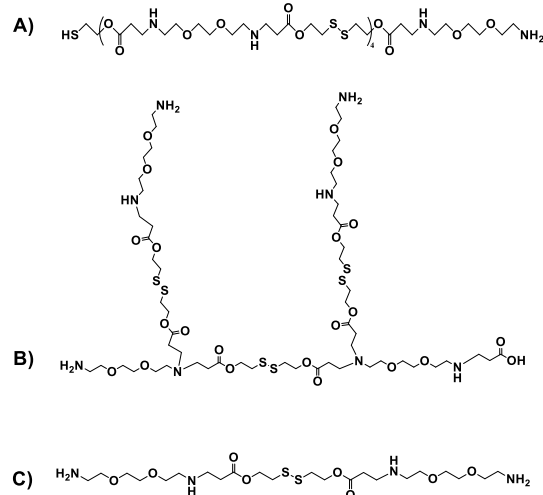


Figure 3: Putative structures of the OBAEs A, B and C based on the most common fragments from mass spectrometry and amine titration data.

Prior papers describing poly(beta-aminoesters) have suggested structures deduced from the molar ratios of the functional groups of the monomers used, and have not always taken into account the potential formation of branches in the polymeric structure, even if diacrylate/diamine monomers have been used.^{28, 29} In our case, we aimed for a variety of structures, including possible branching, such that the oligomers might condense with siRNA in different architectures during the ink-jet printing process.

We next explored the possibility to Inkjet print the oligomers with siRNA. This method has been exploited for biomaterials and drug discovery³⁰⁻³², cell based therapies³³ and for screening amorphous solid dispersions¹¹ but to date only a few examples have been demonstrated for the formulation of micro- and nano- drug delivery systems.³⁴⁻³⁶ We thus screened the capability of the OBAEs to condense with siRNA by ink-jet printing in a 96-well plate starting from aqueous stock solutions of polymers and siRNA at different concentrations (Fig. 4). The amount of siRNA used was minimised by adoption of this method. For example, it was possible to perform 100 different experiments, with nine repeats of each OBAE/siRNA polyplex formulation (at each explored ratio), with as little as 800 ng of siRNA. The use of diluted solution of siRNA (0.01 % w/v) allowed to work with ink formulations presenting low viscosity, close to the one of pure water (video as supporting data). By handling inks with such low viscosity, well-defined droplets were produced. Consequently, it has been simple to prevent the unwanted production of satellite droplets, as showed in Figure S9.

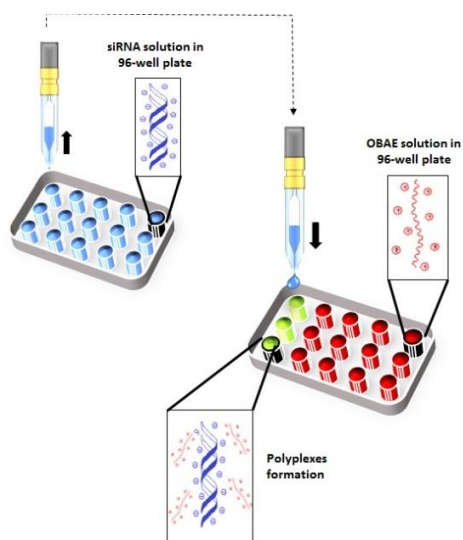


Figure 4. Schematic illustration of OBAE/siRNA polyplexes formation through ink-jet printing technique.

The full set of polyplexes was prepared in less than 20 min by adopting a fully automated loop, and with the further advantage of storing all the samples in the compact space of a single 96-wellplate. The properties of the obtained polyplexes were compared with those made by conventional manual nanoprecipitation routes in order to confirm the potential and the reproducibility of this technique in the formation of drug delivery systems (Fig. S8A-B). Polyplexes at different polymer/siRNA ratios were characterized in terms of size and polydispersity index through dynamic light scattering (DLS) (Fig. 5A). AFM analysis were also carried out, as shown for the OBAE C/siRNA polyplex at polymer/siRNA 10:1 weight ratio to better clarify the morphology, size and shape of the polyplexes. As evident in Fig. 5B, the OBAE/siRNA polyplexes were of spherical shape with size distributions in line with DLS data (between 200 nm and 500 nm).

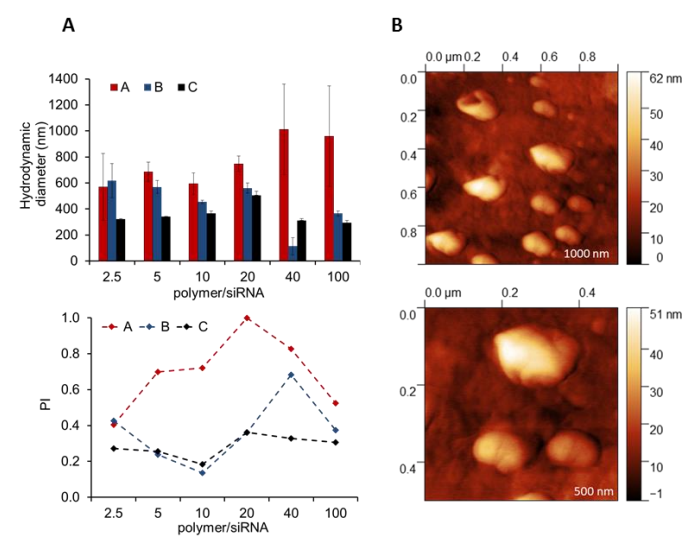


Figure 5. Characterization of OBAE/siRNA polyplexes (A) Size and polydispersity index of OBAE/siRNA polyplexes at different polymer/siRNA weight ratios. (B) AFM images of OBAE C/siRNA polyplex at polymer/siRNA 10:1 weight ratio.

The OBAs were found to exhibit different behaviours in terms of complexation with siRNA, as expected from their chemical structures and charge densities. In particular, OBAE A formed polyplexes ranging from 600 to 1000 nm characterized by high polydispersity indexes, depending on the amount of siRNA condensed. In contrast, OBAE C showed the best performance in terms of complexation, thus forming polyplexes from 200 to 450 nm with an uniform size distribution in all the siRNA concentrations tested.

The ability of the OBAs to form complexes with siRNA was investigated by agarose gel retardation (Fig. 6A) and ethidium bromide displacement assays (Fig. 6B). For the latter experiment, calf thymus DNA was incubated with ethidium bromide for 30 min and thereafter mixed with polyplexes at different polymer/siRNA ratio. Ethidium bromide displacement was monitored by fluorescence spectroscopy. In addition, experiments were carried out to simulate the behaviour of the polyplexes in an intracellular reducing environment. Accordingly, polyplexes were dispersed in buffer solutions containing GSH (10 mM) and their size was monitored throughout 2h of incubation. As apparent from Fig. 6C, a marked change in the median diameters of particles in solution from ~100 nm to ~10 nm was observed after addition of GSH, indicating disassembly of the polyplexes following reductive stimulus.

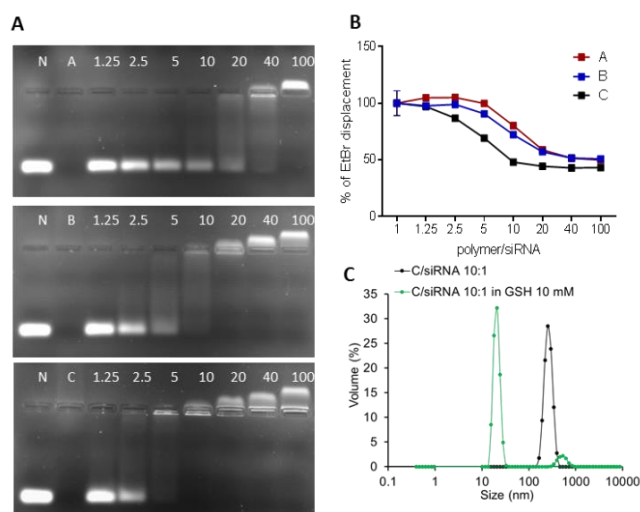


Figure 6. (A) siRNA condensation by A, B and C at different polymer/siRNA weight ratios as evaluated by the gel retardation assay. N represents naked siRNA. (B) Ethidium bromide displacement assay. (C) Stability of PBAE C/siRNA polyplex at polymer/siRNA 10:1 weight ratios incubated in GSH 10 mM for 2h.

The obtained results combined with the gel retention assays, confirmed the different condensation capabilities of OBAs with siRNA, in line with their different charge densities. In particular, it was evident from the dye displacement and gel retardation assays that the siRNA binding affinity per unit mass of OBAs increased from sample A to sample C, and that the polyplexes were disassembled in reducing environments. No significant difference in siRNA condensation capacity of OBAs via jet printing or manual method was found (Fig. S8C). The biological effects of the OBAE-siRNA polyplexes were investigated in A549 lung cancer cells. In this study we designed

disulfide-linked OBAs of intermediate molar mass such that the oligomers would have sufficient charge to associate with siRNA during transit across cellular barriers, but also have an ability to depolymerise rapidly in the reducing intracellular environments to fragments which would have low affinity for siRNA and also low cytotoxicity.^{16, 37, 38} We therefore compared the effects of free OBAs on the metabolic activities of A549 cells to those of the widely-used transfection agent branched PEI (25kDa) after 4 h of treatment (Fig 7A). Gene knockdown was then evaluated in an A549 cell line which constitutively expressed luciferase, using an anti-Luciferase siRNA (CCGCAAGAUCGCGAGAUU) and a control siRNA with a non-coding (scrambled) sequence. Cells were incubated for 4h with OBAE-siRNA polyplexes at OBAE/siRNA 10:1 weight ratio (10 µg/mL of polyplexes) (Fig 7B).

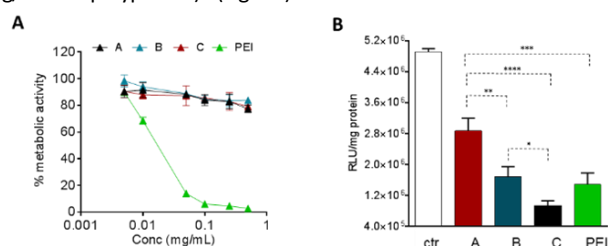


Figure 7: A) Cytotoxicity of free OBAs and B) In vitro luciferase siRNA transfection from polyplexes vs free siRNA (ctr) in A549-luciferase expressing cells after 4h of incubation. RLU= relative light units, a measure for luciferase expression. Results are expressed as mean ± SD of three experiments. ****P<0.0001, ***P<0.001, **P<0.01, *P<0.05 two-way ANOVA test.

The A549 cells retained ~ 80% metabolic activity even when treated with the higher concentration of OBAs and were significantly less toxic compared to PEI, which caused cell death at similar concentrations. As expected from the different siRNA binding properties of the OBAs developed, a progressive increase in transfection efficiency was observed from oligomer A to oligomer C, with an overall knockdown activity of OBAE C greater than that of PEI at the same weight ratio (Fig. 7B), independently by the preparation method (Fig. S8D). The intracellular transport of the polyplexes was probed in preliminary confocal microscopy experiments using a fluorescent Cy3-tagged siRNA (Figure 8). Inspection of the micrographs indicated that a progressive increase in siRNA internalization occurred ranging from oligomer A to oligomer C at the same concentration and time frame, in line with the expected trend based on the transfection results.

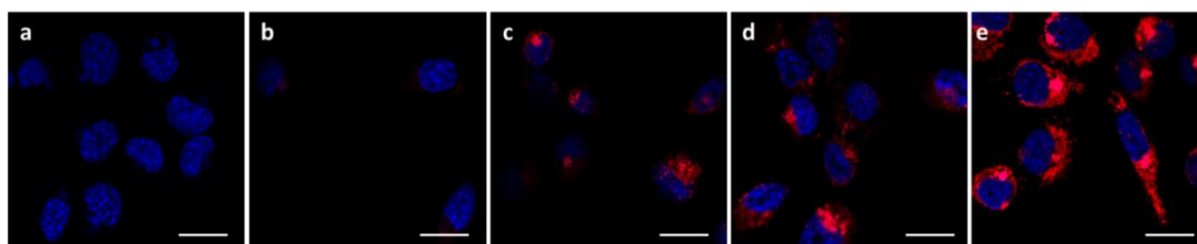


Figure 8: Confocal images of A549-luciferase expressing cells after 4h of incubation with 10 µg/mL of polyplexes. A) Uptake of OBAE/Cy3-siRNA polyplexes at 10:1 polymer/siRNA weight ratio. Cell nuclei were stained with DAPI (blue) and the images were acquired with 545 nm excitation and LP 560 nm spectral filters for Cy3-siRNA detection (red). a) untreated cells, b) naked siRNA, c) OBAE A polyplexes, d) OBAE B polyplexes, e) OBAE C polyplexes. Zen 2009 image Software was utilized for image processing. Scale bar: 20 µm.

The successful knockdown indicated that some of the polyplexes were able to escape to the reducing cytosolic regions where oligomer breakdown enabled delivery of the siRNA. Based on the previously described titration curves, the buffering capacities of the polymers were calculated to be 17, 24 and 56% for OBAE A, B and C respectively. Thus it was expected that OBAE C might be the most effective as an endosomal buffering agent to exploit the 'proton sponge' effect. As apparent from

Figure 9, a partial co-localization of the delivered siRNA with the lysosomes was found for OBAE C, suggesting that these complexes were initially trafficked to endolysosomal compartments. The subsequent enhanced knockdown achieved by these complexes was indicative that the OBAE C polyplexes were more stable in these regions compared to those of A and B, and were hence able to deliver siRNA more effectively following endo-lysosomal escape.

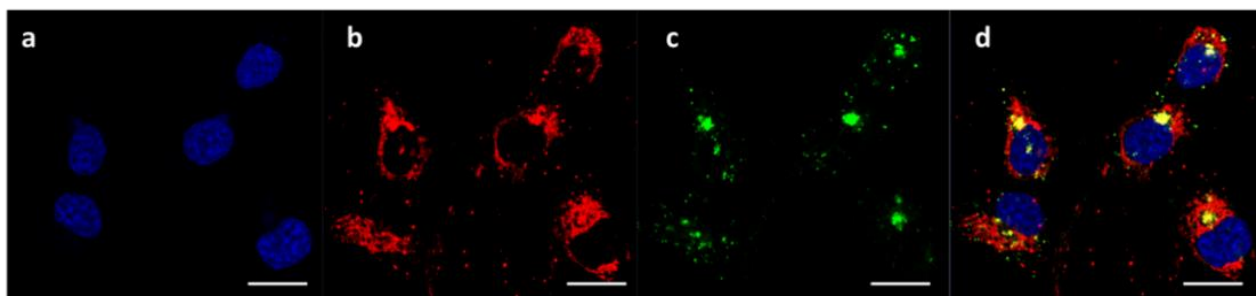


Figure 9: Intracellular trafficking of OBAE C/Cy3-siRNA polyplexes at 10:1 polymer/siRNA weight ratio. a) nucleus stained with DAPI, b) Cy3-siRNA emission (ex: 555 nm excitation, em: LP 560), c) LysoTracker Green DND-26 emission (ex: 488 nm, em: SP 555), d) merge. Zen 2009 image Software was utilized for image processing. Scale bar: 20 µm

The data together indicated that the lowest molar mass OBAE was the most effective in terms of ease of formulation via ink-jet printing, and also in delivering siRNA to knock down the activity of luciferase. Based on NMR and mass spectrometry data, OBAE C was identified as the adduct of 2 ethylene-dioxy-bis-ethylamine monomers bridged by a single DSD unit, and would therefore have the highest number of basic amines per unit mass of the three OBAEs prepared. The titration data confirmed this assertion, and it was thus not surprising that OBAE C was the most effective of the candidates in siRNA condensation and polyplex formation. Our aim in this study was not to optimise the delivery systems, but to identify early in a synthesis/formulation cycle which, out of a pool of potential nucleic acid carriers, might be best from a printing and primary efficacy perspective. The fact that we were able to identify rapidly an oligo-beta-amino ester, which was as active as PEI in transfection but with much reduced effects on metabolic activity, using this method is indicative of its promise for future synthesis and formulation strategies.

Conclusions

Here we have shown the synthesis and characterisation of redox responsive oligo- β -aminoesters for siRNA delivery into cancer cells. Through an appropriate modulation of the molar ratio of the starting materials, we obtained oligo- β -aminoesters with different structures and charge densities. These cationic materials were rapidly condensed with siRNA through a facile and versatile high-throughput inkjet method, thus forming polyplexes with different siRNA binding affinities as well as colloidal properties. The new OBAEs showed reduced toxicity against cancer cells compared to the standard comparator PEI, yet retained a comparable high efficacy for transfection of siRNA in A549 cells. Future work will investigate the *in vivo* activities of these promising materials.

Acknowledgments

Claudia Conte was supported by a fellowship by Associazione Italiana per la Ricerca sul Cancro (AIRC) co-funded by the European Union (iCARE/Marie Curie 2014). Tatiana Lovato thanks the EPSRC for a Doctoral Prize Fellowship. This work was supported by the Engineering and Physical Sciences Research Council grant numbers EP/H005625/1, EP/N03371X/1 and a Royal Society Wolfson Research Merit Award (WM150086) to CA. We also thank Tom Booth, Paul Cooling, Esme Ireson and Christine Grainger-Boulton for technical support.

Data access statement

All raw data created during this research are openly available from the corresponding authors (cameron.alexander@nottingham.ac.uk and claudia.conte@unina.it) and at the University of Nottingham Research Data Management Repository (<https://rdmc.nottingham.ac.uk/>). All analyzed data supporting this study are provided as ESI⁺ accompanying this paper.

Conflicts of interest

There are no conflicts to declare.

References

1. Z. Zhou, X. Liu, D. Zhu, Y. Wang, Z. Zhang, X. Zhou, N. Qiu, X. Chen and Y. Shen, *Advanced drug delivery reviews*, 2017, **115**, 115-154.
2. A. N. Zelikin, C. Ehrhardt and A. M. Healy, *Nat Chem*, 2016, **8**, 997-1007.
3. M. A. Islam, E. K. G. Reesor, Y. Xu, H. R. Zope, B. R. Zetter and J. Shi, *Biomaterials Science*, 2015, **3**, 1519-1533.
4. A. Samanta and I. L. Medintz, *Nanoscale*, 2016, **8**, 9037-9095.
5. D. W. Bartlett and M. E. Davis, *Bioconjugate Chemistry*, 2007, **18**, 456-468.
6. J. C. Kasper, D. Schaffert, M. Ogris, E. Wagner and W. Friess, *Journal of Controlled Release*, 2011, **151**, 246-255.
7. S. C. Semple, A. Akinc, J. X. Chen, A. P. Sandhu, B. L. Mui, C. K. Cho, D. W. Y. Sah, D. Stebbing, E. J. Crosley, E. Yaowski, I. M. Hafez, J. R. Dorkin, J. Qin, K. Lam, K. G. Rajeev, K. F. Wong, L. B. Jeffs, L. Nechev, M. L. Eisenhardt, M. Jayaraman, M. Kazem, M. A. Maier, M. Srinivasulu, M. J. Weinstein, Q. M. Chen, R. Alvarez, S. A. Barros, S. De, S. K. Klimuk, T. Borland, V. Kosovrasti, W. L. Cantley, Y. K. Tam, M. Manoharan, M. A. Ciufolini, M. A. Tracy, A. de Fougères, I. MacLachlan, P. R. Cullis, T. D. Madden and M. J. Hope, *Nature Biotechnology*, 2010, **28**, 172-U118.
8. A. L. Troutier-Thuilliez, J. Thevenot, T. Delair and C. Ladaviere, *Soft Matter*, 2009, **5**, 4739-4747.
9. M. Sanna, G. Sicilia, A. Alazzo, N. Singh, F. Musumeci, S. Schenone, K. A. Spriggs, J. C. Burley, M. C. Garnett, V. Taresco and C. Alexander, *ACS Med Chem Lett*, 2018, **9**, 193-197.
10. I. Louzao, B. Koch, V. Taresco, L. Ruiz-Cantu, D. J. Irvine, C. J. Roberts, C. Tuck, C. Alexander, R. Hague, R. Wildman and M. R. Alexander, *ACS Appl Mater Interfaces*, 2018, **10**, 6841-6848.
11. V. Taresco, I. Louzao, D. Scurr, J. Booth, K. Treacher, J. McCabe, E. Turpin, C. A. Laughton, C. Alexander, J. C. Burley and M. C. Garnett, *Molecular Pharmaceutics*, 2017, **14**, 2079-2087.
12. P. Mastorakos, C. Zhang, E. Song, Y. E. Kim, H. W. Park, S. Berry, W. K. Choi, J. Hanes and J. S. Suk, *Journal of controlled release : official journal of the Controlled Release Society*, 2017, **262**, 37-46.
13. S. Y. Tzeng, D. R. Wilson, S. K. Hansen, A. Quinones-Hinojosa and J. J. Green, *Bioengineering & translational medicine*, 2016, **1**, 149-159.
14. D. G. Anderson, D. M. Lynn and R. Langer, *Angewandte Chemie*, 2003, **42**, 3153-3158.
15. C. G. Zamboni, K. L. Kozielski, H. J. Vaughan, M. M. Nakata, J. Kim, L. J. Higgins, M. G. Pomper and J. J. Green, *Journal of controlled release : official journal of the Controlled Release Society*, 2017, **263**, 18-28.
16. A. A. Eltoukhy, D. J. Siegwart, C. A. Alabi, J. S. Rajan, R. Langer and D. G. Anderson, *Biomaterials*, 2012, **33**, 3594-3603.
17. S. Werth, B. Urban-Klein, L. Dai, S. Hobel, M. Grzelinski, U. Bakowsky, F. Czubayko and A. Aigner, *Journal of controlled release : official journal of the Controlled Release Society*, 2006, **112**, 257-270.

18. J. C. Sunshine, D. Y. Peng and J. J. Green, *Mol Pharm*, 2012, **9**, 3375-3383.
19. F. Martello, M. Piest, J. F. Engbersen and P. Ferruti, *Journal of controlled release : official journal of the Controlled Release Society*, 2012, **164**, 372-379.
20. A. A. Y. Almulathanon, E. Ranucci, P. Ferruti, M. C. Garnett and C. Bosquillon, *Pharmaceutical research*, 2018, **35**, 86.
21. P. Y. Teo, C. Yang, J. L. Hedrick, A. C. Engler, D. J. Coady, S. Ghaem-Maghami, A. J. T. George and Y. Y. Yang, *Biomaterials*, 2013, **34**, 7971-7979.
22. X. J. Deng, N. Zheng, Z. Y. Song, L. C. Yin and J. J. Cheng, *Biomaterials*, 2014, **35**, 5006-5015.
23. A. Akinc, M. Thomas, A. M. Klibanov and R. Langer, *Journal Of Gene Medicine*, 2005, **7**, 657-663.
24. A. Akinc and R. Langer, *Biotechnol. Bioeng.*, 2002, **78**, 503-508.
25. S. Y. Tzeng, B. P. Hung, W. L. Grayson and J. J. Green, *Biomaterials*, 2012, **33**, 8142-8151.
26. K. L. Kozielski, S. Y. Tzeng and J. J. Green, *Chem Commun*, 2013, **49**, 5319-5321.
27. C. Y. Hong, Y. Z. You, D. C. Wu, Y. Liu and C. Y. Pan, *Journal of the American Chemical Society*, 2007, **129**, 5354-5355.
28. J. Kim, J. C. Sunshine and J. J. Green, *Bioconjug Chem*, 2014, **25**, 43-51.
29. A. A. Eltoukhy, D. Chen, C. A. Alabi, R. Langer and D. G. Anderson, *Advanced materials*, 2013, **25**, 1487-1493.
30. D. G. Anderson, S. Levenberg and R. Langer, *Nat Biotechnol*, 2004, **22**, 863-866.
31. E. A. Clark, M. R. Alexander, D. J. Irvine, C. J. Roberts, M. J. Wallace, S. Sharpe, J. Yoo, R. J. M. Hague, C. J. Tuck and R. D. Wildman, *Int J Pharmaceut*, 2017, **529**, 523-530.
32. A. B. M. Buanz, C. C. Belaunde, N. Soutari, C. Tuleu, M. O. Gul and S. Gaisford, *Int J Pharmaceut*, 2015, **494**, 611-618.
33. T. Xu, J. Rohozinski, W. X. Zhao, E. C. Moorefield, A. Atala and J. J. Yoo, *Tissue Eng Pt A*, 2009, **15**, 95-101.
34. T. Ehtezaei, N. M. Dempster, G. D. Martin, S. D. Hoath and I. M. Hutchings, *Journal of pharmaceutical sciences*, 2014, **103**, 3733-3742.
35. S. Hauschild, U. Lipprandt, A. Rumpelcker, U. Borchert, A. Rank, R. Schubert and S. Forster, *Small*, 2005, **1**, 1177-1180.
36. N. Scoutaris, S. Ross and D. Douroumis, *Pharmaceutical research*, 2016, **33**, 1799-1816.
37. H. Y. Xue, S. M. Liu and H. L. Wong, *Nanomedicine-Uk*, 2014, **9**, 295-312.
38. M. Breunig, U. Lungwitz, R. Liebl and A. Goepferich, *P Natl Acad Sci USA*, 2007, **104**, 14454-14459.